HIGH SCHOOL EDITION
Journal of Student Research
Volume 14 Issue 1 (2025)

Quantifying Doxorubicin Toward Adaptive Chemotherapy with an Electrochemical Aptamer-Based Biosensor

Emma Chang[1], Arin Kathapurkar[2], Ya Ma[3] and Jason Lee[#]

[1]Lynbrook High School, USA
[2]Bellarmine College Preparatory, USA
[3]Aiglon College, USA
[#]Advisor

ABSTRACT

Despite more than 100 chemotherapy treatments being available worldwide, 10 million people died of cancer in 2023. Doxorubicin is a common chemotherapy treatment, yet its survival rate is 28% due to its narrow therapeutic window, suggesting cardiotoxicity if slightly overdosed and insufficient anti-cancer effects if underdosed. These statistics highlight the flaws in current chemotherapy regimens, demanding a need for more effective treatment methods. Current chemotherapy dosing calculations do not account for the fact that each patient's drug response can vary up to ten-fold, stressing the importance of adaptive and personalized dosing for effective treatment. This study outlines the platform framework for an intravenous biosensor to monitor the concentration of doxorubicin using an aptamer as its biorecognition element. Existing sequences determined via SELEX were used to generate an oligonucleotide library of aptamers. These aptamers were further engineered to maintain high affinity while undergoing conformational changes in blood. Computational methodologies and analysis techniques were used to simulate molecular docking. This sensing platform is intricately designed to monitor the concentration of doxorubicin in cancer patients toward effectively tailoring chemotherapy regimens to each patient.

Introduction

In 2023, approximately 20 million new cancer cases were reported worldwide, a figure that is expected to rise 57% by 2040, implicating the need for effective treatment plans[1]. Chemotherapeutics work by inducing apoptosis within cancer cells[2]. However, their narrow therapeutic windows prove problematic as slightly overdosing can damage healthy cells and underdosing results in insufficient anti-cancer effects[3]. Anthracyclines such as doxorubicin (Figure 1) are some of the strongest chemotherapy drugs known for their cytotoxic side effects, warranting a cumulative treatment dose limit[4]. Doxorubicin is used to treat a variety of cancers including sarcomas, metastatic cancers, and breast cancer[5]. However, it introduces cardiogenic, mutagenic, and cardiotoxic side effects alongside its anti-cancer benefits[6].

Broadly, doxorubicin induces apoptosis through three main pathways: intercalation with DNA, inhibition of Topoisomerase II, and the creation of free radicals[7]. Although the exact mechanism of the doxorubicin's intercalation is not fully understood, each part of its structure plays a unique role: the anthraquinone ring is responsible for the hydrogen bonding between the base pairs and doxorubicin, while the daunosamine sugar binds to the minor groove of the DNA[8] (Figure 1).

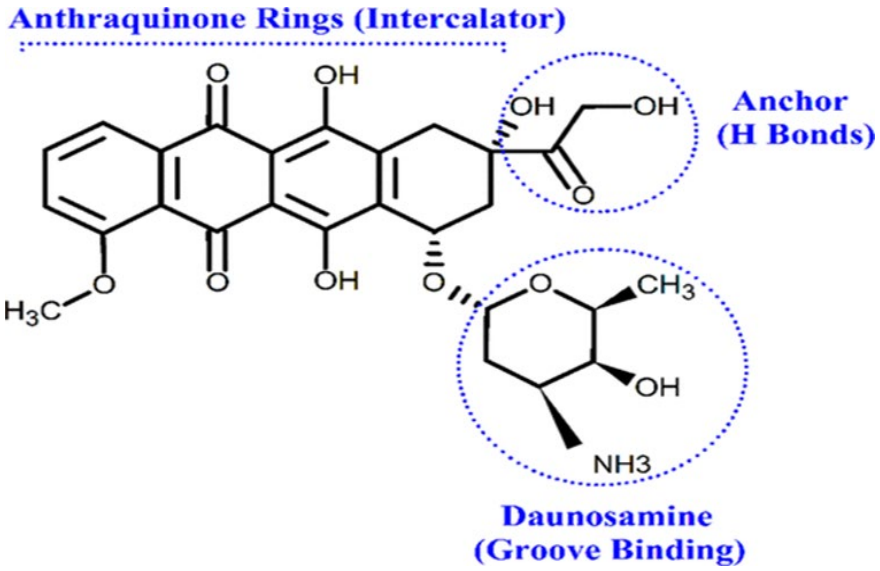

Figure 1. Each part of doxorubicin's chemical structure contributes to its ability to intercalate with DNA. The anthraquinone rings go between the base pairs while the anchor forms hydrogen bonds with the base pairs. Daunosamine binds to the minor groove of DNA[8].

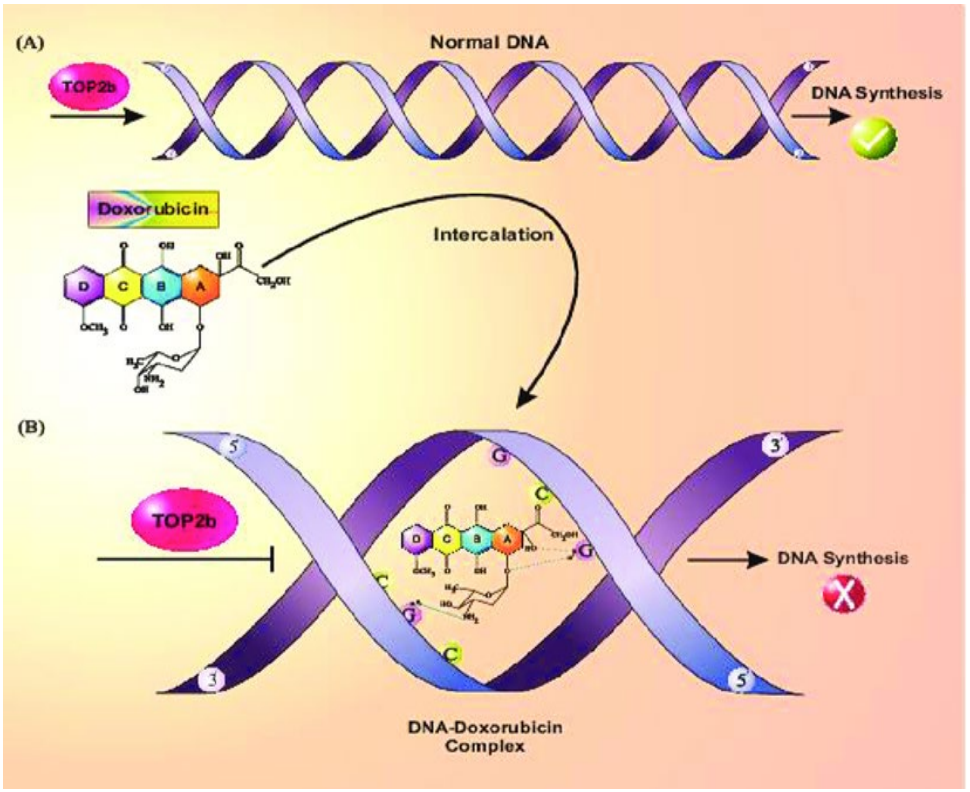

Figure 2. Doxorubicin works by inserting itself between the base pairs of DNA, otherwise known as intercalation with DNA. Part (A) depicts normal DNA synthesis, in which topoisomerase II unwinds the DNA preparing it for replication. Part (B) shows how doxorubicin inserts itself between the base pairs of DNA, causing torsional stress on the DNA and inhibiting topoisomerase II, thus causing a failure in DNA synthesis[9].

In addition to causing torsional stress and nucleoside eviction, intercalation may also inhibit Topoisomerase II from stabilizing the DNA during replication, thus inducing apoptosis (Figure 2)[9]. The main way in which doxorubicin causes cardiotoxicity is through free radicals, which can't be fought off by cardiomyocytes since they lack superoxide dismutase, which is an enzyme used to neutralize free radicals. Free radicals can form both as doxorubicin reacts with iron to form hydroxyl radicals as the quinone rings are oxidized[10]. However, doxorubicin does not solely target cancerous cells and can cause damage throughout the body, meaning that the drug has potential to cause permanent damage if overdosed in patients due to its tendency to kill healthy cells as well[11].

An appropriate administration of doxorubicin is crucial to the recovery of cancer patients because the severity of its detrimental side effects increases if the dosage of doxorubicin exceeds the therapeutic window. On the contrary, there is significant reduction in anti-cancer benefits when underdosed. However, current body-surface area calculations do not account for the high degree of interpatient and intrapatient pharmacokinetic variability seen in doxorubicin metabolism[3]. Furthermore, Rudek et. al found a 30.6% coefficient of variability for interpatient doxorubicin elimination after body-surface area based dosing[12]. As medicine advances, such generalizations no longer suffice, necessitating a dosing methodology that accounts for individual responses to treatment.

Currently hospitals manage doxorubicin treatment through lab-based tests which rely on blood or urine samples[13].

Recent advances in point of care sensing for doxorubicin with the development of DNA-based lateral flow assays still rely on collecting urine samples, which can be a timely process, creating delay between testing results and clinical decision making for drugs[14]. In order to answer the need for rapid, feedback-based doxorubicin dosing, this study proposes an electrochemical aptamer-based biosensor that monitors doxorubicin concentrations in real time, enabling doctors to use pharmacokinetic data of doxorubicin to create patient specific drug regimens.

The sensor is designed to be a bedside monitor with the electrodes inserted into the patient's bloodstream via a catheter (Figure 5). Since doxorubicin is administered through the bloodstream[15], our sensor is situated intravenously to monitor changes in concentration over time. Although this model is more invasive than sensors based in the interstitial fluid, being able to quantify concentrations of doxorubicin in the bloodstream gives an idea of how well the body is up taking the drug[16], thus providing an evaluation on how effective the dosage is.

Our biorecognition element is an aptamer, a single-stranded DNA sequence engineered to have a high affinity for its target ligand. For an electrochemical sensor, in the presence of its target, the aptamer will undergo a structure switch which can be detected by the electrode through signaling from the reporter molecule attached to the aptamer[17]. These reporter molecules include a fluorophore and quencher system or a redox reporter, which ultimately generate a signal after the aptamer undergoes a conformational change (structure switch)[18].

Aptamers have multiple advantages in real-time sensing platforms when compared to other biorecognition elements such as antibodies and enzymes. The main disadvantage of antibodies is that they have a high avidity[19], making it unlikely to unbind their target, resulting in difficulty monitoring concentrations of the analyte. Additionally, creating new antibodies can be costly as they are made in animal models[20]. Enzymes are highly specific, can react with the target, and are far too complex to synthesize with current technologies[21]. However, aptamers can be synthesized through Sequential Evolution of Ligands by EXponential Enrichment (SELEX) which allows them to be as sensitive or specific as necessary for the application[22].

Wochner et al.[23] performed SELEX for daunomycin[24], a molecule similar in structure to doxorubicin, with the magnetic bead procedure. Biotinylated daunomycin is attached to streptavidin-coated magnetic beads which are used to find the binding sequences in a library with over 10^{14} oligonucleotides. This process is repeated to ensure that derived sequences have a high affinity for their target. Although our aptamer was originally designed for daunomycin,

a competitive assay test shows that our sequence had a stronger affinity for doxorubicin[23]. This is likely due to the fact that doxorubicin has an hydroxyl group in the region where it binds to the aptamer, causing stronger hydrogen bonds than daunomycin.

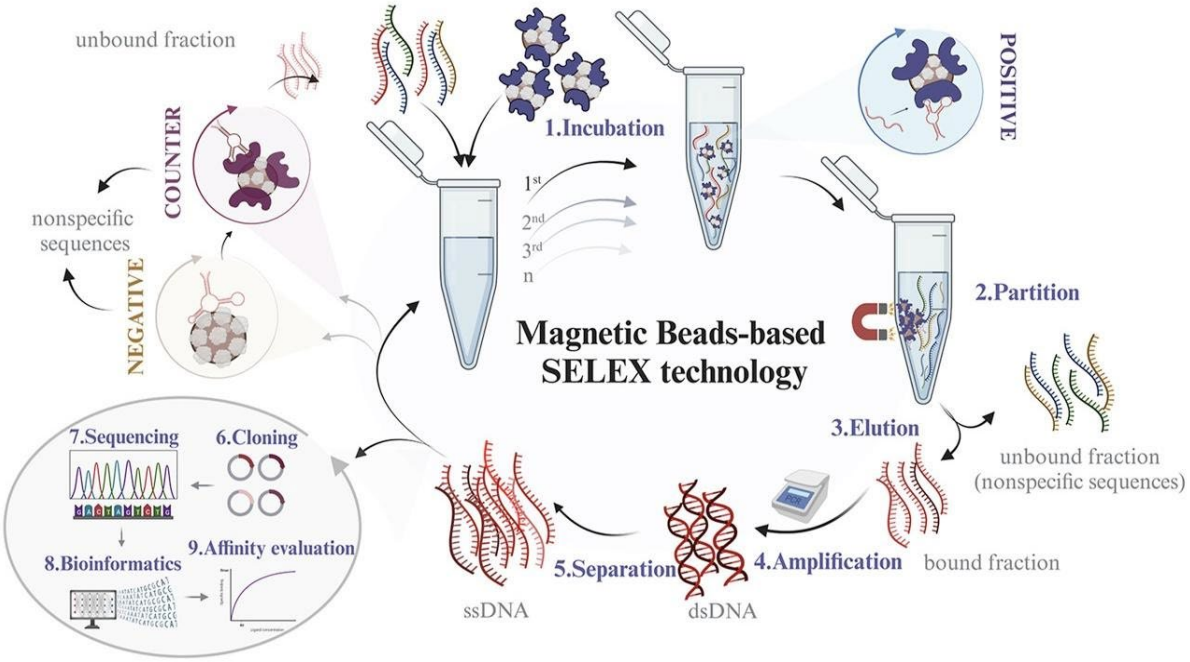

Figure 3. Schematic outline of magnetic beads SELEX, which was used to find our aptamer sequence. (1) Magnetic beads prepared with daunomycin are incubated with oligonucleotides to find sequences that bind. (2) Magnetic separator used to separate the beads with bound sequences from the unbound sequences. (3) Elution used to keep the binding sequence and wash away the unbound sequences. (4) PCR is used to amplify the DNA and make copies of the binding sequences. (5) The double stranded DNA (dsDNA) is separated into its single stranded version (ssDNA). The whole process is then repeated multiple times depending on how specific the aptamer needs to be[24].

This study engineers aptamer sequences for the proposed electrochemical aptamer-based biosensor to monitor intravenous concentrations of doxorubicin using the parent aptamers derived from SELEX. The sensor's real-time pharmacokinetic data on each patient's metabolic response to doxorubicin will help doctors make rapid decisions on adjustments in therapy, thus bridging personalized medicine with chemotherapy regimens.

Methodology

Generating the Aptamer Library

After deriving the parent aptamer and the variable site through SELEX (Figure 3), we created an aptamer library with UNAfold[25], Alpha Fold[26], PyMOL[27], and DockingPie[28]. To serve as an effective biorecognition element, it is essential that the chosen aptamer sequence undergoes a conformational change in the presence of the target in intravenous conditions. We used UNAfold to truncate the aptamer sequences, to ensure that the aptamer would be destabilized, or unfolded, in the absence of target molecules and folded in its presence. This is important because the structure switching allows the electrode to give feedback about the redox reporter. If the aptamer is not destabilized, it would remain in one state (folded or unfolded) regardless of whether the target appears in the environment, making it impossible for

the biosensor to detect changes in concentration. To ensure each aptamer met this criteria, we made truncations to minimize the free energy of the folded state of the sequences by deleting parts of or making base pair substitutions. We took blood temperature, pH, and electrolyte concentrations into account while making truncations to ensure that our aptamer would work while situated intravenously (37°C [29], 140mM Na^{+} [30], 2mM Mg^{2+} [31]). Changing these parameters can adversely affect the aptamer, decreasing its binding affinity for its target or causing misfolding or denaturation, leading to inaccurate results[17].

Molecular Docking

In order to validate that our truncations did not adversely affect the binding of our sequences, we modeled the tertiary structure of our aptamer sequences and doxorubicin with computational models. We used Alpha Fold, PyMOL, and DockingPie which are 3-dimensional platforms to create protein structures, to model biological macromolecules with molecular-level detail in a 3-dimensional environment, and to simulate the docking of target ligands to their receptors respectively. Alpha Fold was utilized to generate the most likely tertiary structure of our aptamer sequences and PyMOL to visualize them with doxorubicin. Although this helped us visually confirm the existence of a binding site on each of our aptamer sequences, we used DockingPie to run a molecular docking simulation for all the sequences in the library to ensure this. Using Autodock Vina[32,33], a docking program in the DockingPie plugin, we simulated ten different binding poses for each sequence, and verified the presence of a likely binding site on each aptamer despite our modifications to the parent sequence.

Results

Electrochemical Aptamer-Based Sensing Platform

Our electrochemical aptamer-based (EAB) sensor is specifically designed for bedside applications and real-time monitoring of doxorubicin in a patient's bloodstream. The sensor consists of a working, reference, and counter electrode which are packed into a catheter that goes into the patient's bloodstream (Figure 5). The biorecognition element, aptamers, are attached to the gold working electrode by a thiol group on the 5' end of the aptamer sequence.

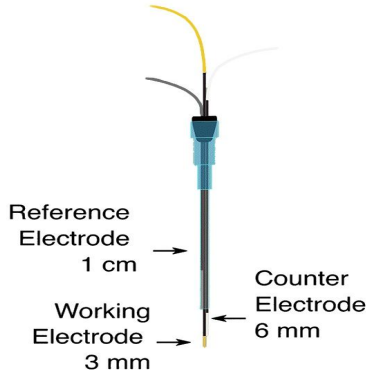

Figure 4. A schematic diagram with the different electrodes of the biosensor packaged within the catheter, adapted from Leung et. al[34].

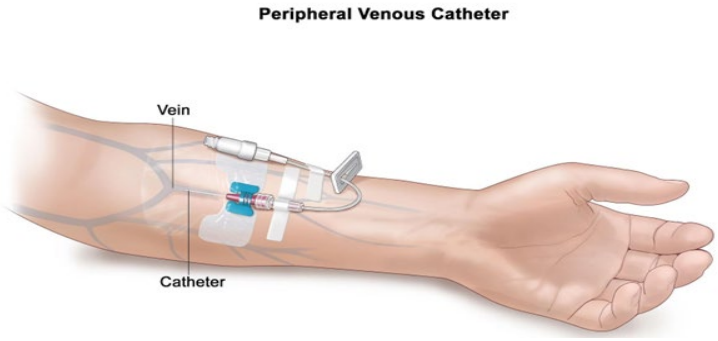

Figure 5. This diagram depicts the complete bedside setup of the biosensor and how it is inserted intravenously in the forearm[35].

Methylene blue, a widely used redox reporter, is attached to the 3' end of the aptamer to act as a redox reporter that transfers electrons to the working electrode. Upon binding to its target, the aptamer sequence undergoes a conformational change which brings the methylene blue closer to the working electrode, thereby increasing the rate of electron transfer between methylene blue and the surface of the gold, creating a target-dependent change in current when interrogated with square wave voltammetry (Figure 6)[36]. The working electrode is prepared through roughening which increases its surface area, creating more binding sites for aptamers and thus improving the sensor's performance[37]. It is then coated in 6-mercaptohexanol to form a self-assembled monolayer that immobilizes the attached aptamer sequences[38]. The counter electrode is made of inert metal, such as platinum,l and is used to deposit the electrons from the working electrode[39] to complete the circuit while the silver reference electrode provides the working electrode with a zero as a baseline[40].

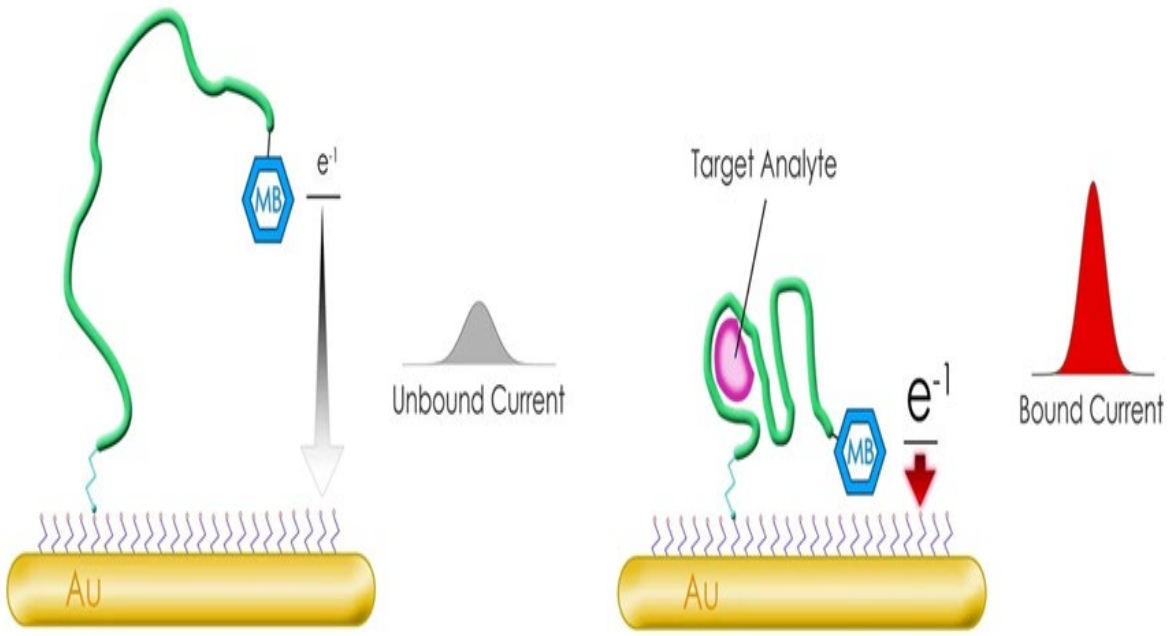

Figure 6. The presence of the target causes the aptamer to undergo a conformational change, causing an increase in electron flow from methylene blue to the working electrode, which generates the change in signal for the bound state shown by the potential vs current curve[36].

The proposed biosensor depends heavily on the aptamer's ability to undergo a conformational change under intravenous conditions when it binds to its target in addition to the specificity of the aptamer to doxorubicin. Following the SELEX process, three aptamer sequences were identified in the parent library (Table 1). Although sequence 10.10 showed the highest affinity for daunomycin throughout the SELEX process, sequence 10.10v is a truncated version of 10.10 that excludes the primer regions on the ends of the sequence, and still demonstrates a comparable affinity for doxorubicin. Sequence 10.10q is the G-rich sequence of 10.10 that was used to identify if G-rich quadruplexes were used in binding of daunomycin[23]. However, 10.10q showed a significant decrease in binding with doxorubicin, which is the main priority while choosing an aptamer sequence for a biosensor. While choosing between sequence 10.10 and 10.10v, we prioritized the free energy of the folded states and the formation of a hairpin structure. This was to ensure that the aptamers would undergo a conformational change when bound to the target (Figure 6) because their affinities were comparable. We chose 10.10v as the parent aptamer for the library of sequences because the truncations of the primer sequences decreased the free energy, by -3.58 kcal/mol.

Table 1. Parent sequences 10.10, 10.10v, and 10.10q which are the sequence with the highest affinity, variable region sequence, and the G-rich truncated sequence respectively. The bolded region of sequence 10.10 is the variable region (10.10v) and the unbolded are the primers that were not necessary for binding[23].

Sequence Name	Sequence
10.10	GGGAATTCGAGCTCGGT**ACCATCTGTG-TAAGGGGTAAGGGGTGGGGGTGGGTAC-GTCT**AGCTGCAGGCATGCAAGCTTGG
10.10v	ACCATCTGTGTAAGGGG-TAAGGGGTGGGGGTGGGTACGTCT
10.10q	AGGGGTAAGGGGTGGGGGTGGGT

After deciding to base most of our aptamer library off base pair truncations from 10.10v, we modeled our aptamer sequences with UNAfold to ensure that the sequences would undergo a conformational change under intravenous conditions of 140mM sodium[30], 2mM magnesium[31], and 37°C[29]. To do this we minimized the free energy of the folded state of the aptamer, which ensures that neither the folded nor unfolded state is heavily favored, thus increasing the likelihood of a target binding induced conformational change. Additionally, we aimed to have the aptamer fold into a hairpin structure (Figure 8), which has been proven to foster the smooth transfer of electrons from the redox reporter to the surface of the gold electrode by keeping the reporter molecule close to the surface of the working electrode[41]. Using this methodology, we generated an aptamer library derived from sequence 10.10v and included other truncated sequences from existing literature[23].

Table 2. The modified sequences in our aptamer library obtained from truncating the variable site and the full sequence with primers. Sequence 10.01vT8A3 was obtained from Ou et al[42]. The naming convention is based on what modifications we made to each sequence: 10.10v denotes the fact that we used sequence 10.10v as the parent aptamer for our library, "T" stands for truncated, and "A" stands for added. The numbers that follow "T" and "A" denote how many base pairs were truncated or added respectively. The free energy of the folded state was obtained from UNAfold simulations and the affinity for the best binding site was determined through molecular docking simulations on DockingPie.

Name	Sequence	ΔG (kcal / mol)	Reason for not choosing	Affinity for Best Binding Site (kcal / mol)
10.10vT13	**ACCATCTGTG-TAAGGGG-TAAGGGGTGGG**	**0.07**	**Chosen**	-7.0
10.10vT14A3_a	GACCATCTGTG-TAAGGGG-TAAGGGGTGGTG	-0.9	Free energy	-8.5
10.10vT14A3_ b	AACCATCTGTG-TAAGGGG-TAAGGGGTGGTG	-0.79	Free energy	-8.0
10.10vT8A3	TGTAAGGGG-TAAGGGGTGGGGGTGGGTACGTCTAGA	0.81	Bad Hairpin	-7.6
10.10vT3A1	GCCATCTGTG-TAAGGGG-TAAGGGGTGGGGGTGGGTACG	-0.31	Hairpin	-8.1
10.10vT6A1	GCCATGTGTG-TAAGGGG-TAAGGGGTGGGGGTGGGT	-0.51	Hairpin	-7.5
10.10vT22	TGTGTAAGGGG-TAAGGGGT	1.8	Not forming a hairpin, unlikely to be in unfolded state	-6.6

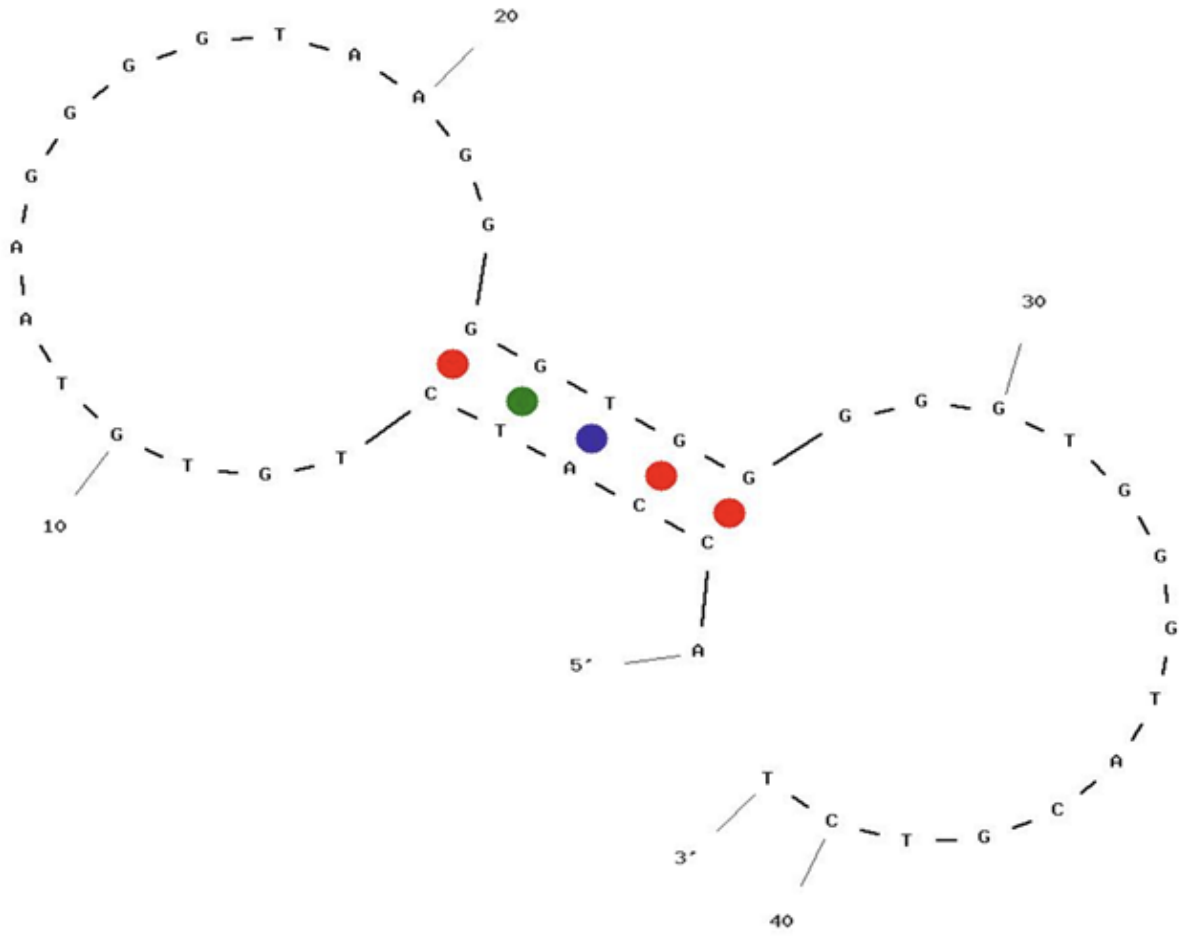

Figure 7. UNAfold was used to predict the folding of the aptamer sequence under intravenous conditions. Parent sequence 10.10V that folds into a dumbbell-like structure and has a folded state free energy of 0.07 kcal/mol under intravenous conditions.

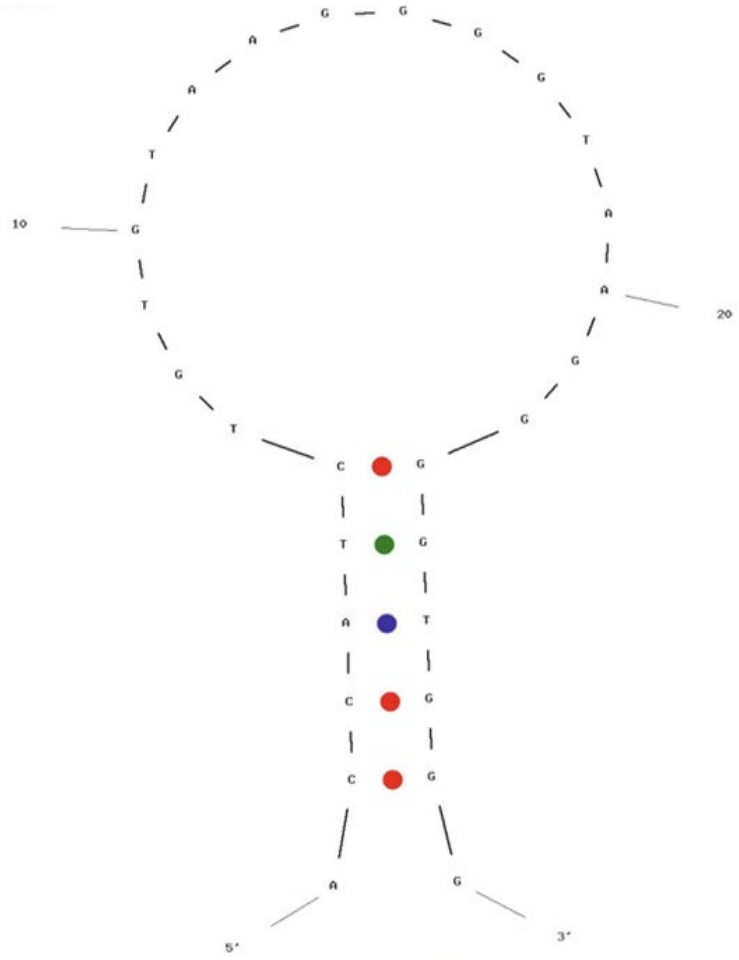

Figure 8. Sequence 10.10T13 that achieves the same folded state free energy as sequence 10.10v and also has a hairpin structure that allows for the transfer of electrons from the redox reporter on the 3' end to the working electrode with minimal sensor noise.

While finalizing an aptamer sequence to use as our biorecognition element, we took the folded structure and free energy of the folded states into account. The folded structure is important to ensure that the conformational change results in a higher rate of electron transfer from the redox report on the 3' end of the aptamer. The ideal hairpin structure in (Figure 8) fosters the smooth flow of electrons from the redox reporter to the electrode. On the contrary, the untruncated parent aptamer depicted in (Figure 7) folds into a dumbbell-like structure, resulting in sensor noise because the aptamer can move around while in its folded state. The second factor in our decision between sequences was the magnitude of the folded state's free energy. Minimizing the magnitude of the free energy is important because a free energy close to zero indicates that the aptamer can easily undergo a structure switch in the presence of the target, because neither the folded state nor unfolded state is heavily thermodynamically favored. While picking sequences in our aptamer library we went with 10.10vT13 because it had both a single hairpin structure and the best free energy.

We used DockingPie 1.2 to simulate the binding interaction between our aptamer and doxorubicin and generate the associated binding free energies. Since the parent aptamer's affinity for doxorubicin was verified through testing, the binding free energy given by the molecular docking simulation (-7.2 kcal/mol) can serve as a benchmark for proving the existence of a binding site on the truncated sequences. Although the truncations slightly lowered the binding free energy (-7.0 kcal/mol), the magnitude of this difference is small enough to conclude that there is a valid binding site on the truncated aptamer sequence. Since we found higher binding free energies for structures such as

10.10vT14_a and 10.10vT14_b which also fold into single hairpins, these sequences could serve as alternatives to test against our chosen aptamer sequence during in vivo testing.

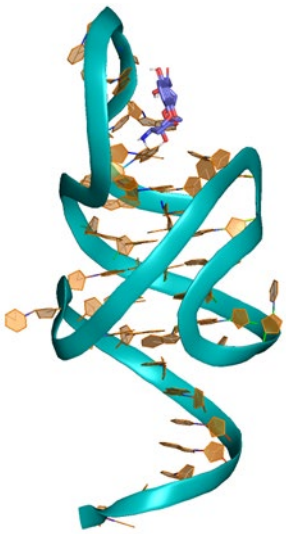

Figure 9. 3-dimensional visualizations of the docking of doxorubicin to the parent aptamer sequence, 10.10v.

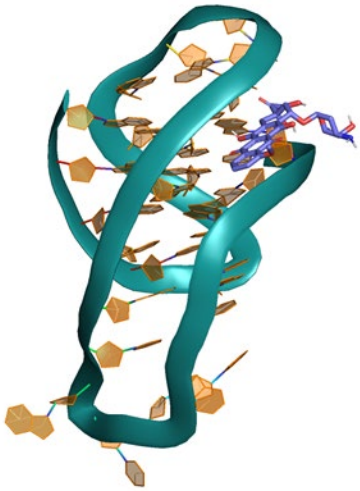

Figure 10. 3-dimensional visualizations of the docking of doxorubicin to the truncated aptamer sequence, 10.10vT13.

We obtained binding free energies of both of these interactions, -7.2 kcal/mol and -7.0 kcal/mol for the parent and truncated sequence respectively and compared them to ensure that after the truncations there was still a valid binding site.

Electrochemical aptamer-based sensors that monitor their target intravenously are subject to sensor drift due to a variety of reasons. Most notably, large molecules in the blood and the degradation of the monolayer on the working electrode of the sensor over time were found to be two of the largest factors in causing sensor drift in real-time monitoring applications[43]. To circumvent this, sensors such as MEDIC utilize a continuous flow diffusion filter that only allows small molecules such as doxorubicin to come in contact with the sensor while preventing other proteins in the blood from fouling the result[44]. However, this method requires the injection of a buffer solution to create laminar flow of the buffer and the bloodstream, adding an additional layer of complexity that would be inconvenient in our bedside

monitoring system. Instead, our sensor accounts for drift through its generation of kinetic differential measurements (KDM) described by Downs et al[45]. To obtain KDM, concentrations of target are added in vitro to the biosensor to generate a signal on and signal off frequencies in which the current increases and decreases in response to target, respectively (Figure 9 & 10). By repeating this process for multiple concentrations of target a calibration curve is generated that accounts for sensor drift.

Feedback Control for Real Time Drug Monitoring

A patient's metabolic response to a chemotherapy drug may vary up to ten-fold[46]. Ensuring that each patient receives a dosage within their target range, especially for exceptionally potent drugs like anthracyclines, is crucial in minimizing cytotoxic and mutagenic side effects of chemotherapeutics. Our biosensor system builds on current studies of feedback-based dose adjustments as it employs a proportional integral (PI) controller, utilized in a Mage et al.[47] to maintain the ideal dosage for each patient. Using the concentrations measured by the biosensor, the proportional term, or K_p, determines the magnitude of the error between the drug concentration in vivo and the target drug concentration (setpoint) whilst the integral term determines the accumulation in this error over time[47]. *In vivo* testing of this feedback model has been exceptionally successful, with the feedback loop system (biosensor-PI controller-drug pump) reaching the setpoint within 10 minutes[47].

$$U(t) = Kpe(t) + Ki\int_0^t e(\tau)\,d\tau$$

Equation 1. PI Controller for Drug Dosage Adjustment. U(t) is the amount of drug that needs to be added/lost to hit the target concentration, e(t) is the error between the known drug concentration and drug concentration at the site of the tumor. K_p and K_i are the proportional and integral terms that are adjusted based on the model of interest[47].

Discussion & Conclusion

Through several computational models and 3-dimensional simulations for electrochemical aptamer-based biosensor, our optimized aptamer effectively addresses the issue of doxorubicin's detrimental side effects due to improper chemotherapy dosing intra and inter patient by producing real time measurements of doxorubicin concentrations to allow for personalized dosage adjustments during chemotherapy.

We designed the sensor with intention to monitor doxorubicin concentrations in real time, by choosing an aptamer as our biorecognition element. Aptamers are single-stranded DNA sequences that have high affinity and specificity for their target. Wochner et al[23] used SELEX to generate a parent library of aptamer sequences with a high affinity for doxorubicin. However, this library of sequences did not contain an optimal sequence specifically for our sensor. Therefore, we modified the base sequences to enable structure switching under intravenous conditions. After performing molecular binding simulations to determine the most-likely binding site for each sequence in our library of possible aptamers, we picked one sequence for our biosensor that theoretically showed the most promising dissociation constant.

While our sensor, with a dissociation constant of 272nM[23], is successful in theory, several factors of in vivo conditions can confound our results by causing sensor drift. Electrochemical aptamer-based biosensors typically have issues when monitoring analytes intravenously due to the presence of high-molecular weight molecules that obstruct binding sites[43]. Overtime, the monolayer on the gold working electrode of our sensor is subjected to degradation from the current flow from methylene blue, our redox reporter[48]. To correct for sensor drift, our platform uses kinetic differential measurements and standard calibration curves to account for sensor drift via software adaptations[47].

Another adaptation for future steps is to test for analogs, which are molecules that are structurally similar to our target doxorubicin[49]. Since doxorubicin is a chemotherapy drug that intercalates with DNA it is essential that our biosensor can differentiate between doxorubicin and other chemotherapy drugs with similar mechanisms that are administered throughout a patient's chemotherapy treatment. Some examples include daunorubicin, idarubicin, and epirubicin[50]. Considering the doxorubicin's metabolite doxorubicinol is essential because it is vastly similar to doxorubicin in structure[51]. Doxorubicin's mechanism as a chemotherapy treatment involves a certain percentage of the initial dosage being excreted from the body unchanged after approximately 5 days[51]. About 45% to 52% of the drug's initial dosage is transformed into metabolite, and around 3% of this amount is turned into doxorubicinol[51]. Chemotherapy treatments with doxorubicin are cumulative, meaning that a certain concentration of doxorubicin lingers in the body even several days after the injection[51]. Throughout the treatment, the metabolite concentration of doxorubicinol accumulates in addition to doxorubicin being injected[51]. To further test the specificity of our sensor, ensuring that our sensor can differentiate between doxorubicin and its analogs, one being doxorubicinol is essential because both can cause adverse side effects.

Our sensor has applications within the future of targeted drug delivery. Bavi et al developed an aptamer-doxorubicin conjugate with a high affinity for Annexin A1 (ANXA1), a protein expressed in tumor vasculature for most cancers[52]. The conjugate demonstrated a 15% increase in tumor growth inhibition rate when compared to free doxorubicin whilst maintaining similar change in tumor volumes in mice models[52]. Additionally, the conjugate demonstrated lower cytotoxicity when compared to the free drug due to the slow release of doxorubicin from the conjugate in the absence of ANXA1[52]. With doxorubicin's survival rate being a mere 28%[53], our electrochemical aptamer-based biosensor allows us to tackle the ineffective dosing mechanisms of chemotherapy. By obtaining real-time data on doxorubicin concentrations in targeted drug delivery models, our sensor has the potential to provide useful insights into the pharmacokinetics of such models to further evaluate their effectiveness.

Acknowledgments

We would like to thank University of California Santa Barbara Summer Research Academies program staff, Dr. Lina Kim, Dr. Teresa Holden for the opportunity to conduct this research and our professors Shaylee Larson and teaching assistant Nicole Emmons and research mentor Sarah Segrave for their guidance and support throughout this entire program.

Author Contribution Statement

Y.M wrote the first draft of the introduction which was later revised by E.C and A.K. A.K and E.C worked together on the methodology and discussion/conclusion sections. A.K wrote the results section which was reviewed by E.C. Y.M and tabulated the figures. E.C worked on the references.

References

(1) Pan American Health Organization. *World Cancer Day 2023: Close the care gap - PAHO/WHO | Pan American Health Organization*. www.paho.org. https://www.paho.org/en/campaigns/world-cancer-day-2023-close-care-gap#:~:text=Globally%2C%20there%20were%20an%20estimated.
(2) Pfeffer, C. M.; Singh, A. T. K. Apoptosis: A Target for Anticancer Therapy. *International Journal of Molecular Sciences* **2018**, *19* (2), 448. https://doi.org/10.3390/ijms19020448.

(3) Gurney, H. How to Calculate the Dose of Chemotherapy. *British Journal of Cancer* **2002**, *86* (8), 1297–1302. https://doi.org/10.1038/sj.bjc.6600139.

(4) American Cancer Society. *How Does Chemo Work? | Types of Chemotherapy*. www.cancer.org. https://www.cancer.org/cancer/managing-cancer/treatment-types/chemotherapy/how-chemotherapy-drugs-work.htm.

(5) Johnson-Arbor, K.; Dubey, R. *Doxorubicin*. PubMed. https://www.ncbi.nlm.nih.gov/books/NBK459232/#:~:text=Doxorubicin%20may%20be%20used%20to.

(6) *Error*. www.bccancer.bc.ca. http://www.bccancer.bc.ca/drug-database-site/Drug%20Index/Doxorubicin_monograph.pdf.

(7) Volkova, M.; Russell, R. Anthracycline Cardiotoxicity: Prevalence, Pathogenesis and Treatment. *Current Cardiology Reviews* **2012**, *7* (4), 214–220. https://doi.org/10.2174/157340311799960645.

(8) Jawad, B.; Poudel, L.; Podgornik, R.; Ching, W.-Y. Thermodynamic Dissection of the Intercalation Binding Process of Doxorubicin to DsDNA with Implications of Ionic and Solvent Effects. *The Journal of Physical Chemistry B* **2020**, *124* (36), 7803–7818. https://doi.org/10.1021/acs.jpcb.0c05840.

(9) Mobaraki, M.; Faraji, A.; Zare, M.; Manshadi, H. R. D. Molecular Mechanisms of Cardiotoxicity: A Review on Major Side-Effect of Doxorubicin. *Indian Journal of Pharmaceutical Sciences* **2017**, *79* (3). https://doi.org/10.4172/pharmaceutical-sciences.1000235.

(10) Yang, F.; Teves, S. S.; Kemp, C. J.; Henikoff, S. Doxorubicin, DNA Torsion, and Chromatin Dynamics. *Biochimica et Biophysica Acta (BBA) - Reviews on Cancer* **2014**, *1845* (1), 84–89. https://doi.org/10.1016/j.bbcan.2013.12.002.

(11) *Doxorubicin (Intravenous Route) Side Effects - Mayo Clinic*. www.mayoclinic.org. https://www.mayoclinic.org/drugs-supplements/doxorubicin-intravenous-route/side-effects/drg-20063553?p=1#:~:text=Doxorubicin%20belongs%20to%20the%20group

(12) Rudek, M. A.; Sparreboom, A.; Garrett-Mayer, E.; Armstrong, D. K.; Wolff, A. C.; Jaap Verweij; Baker, S. D. Factors Affecting Pharmacokinetic Variability Following Doxorubicin and Docetaxel-Based Therapy. *PubMed* **2004**, *40* (8), 1170–1178. https://doi.org/10.1016/j.ejca.2003.12.026.

(13) *Chemotherapy tests*. www.cancerresearchuk.org. https://www.cancerresearchuk.org/about-cancer/treatment/chemotherapy/planning/chemotherapy-tests#:~:text=Some%20chemotherapy%20drugs%20can%20affect.

(14) Pomili, T.; Gatto, F.; Pompa, P. P. A Lateral Flow Device for Point-of-Care Detection of Doxorubicin. *Biosensors* **2022**, *12* (10), 896. https://doi.org/10.3390/bios12100896.

(15) *Doxorubicin (Intravenous Route) Proper Use - Mayo Clinic*. www.mayoclinic.org. https://www.mayoclinic.org/drugs-supplements/doxorubicin-intravenous-route/proper-use/drg-20063553?p=1#:~:text=This%20medicine%20is%20given%20through.

(16) Wang, M.; Lin, J.; Gong, J.; Ma, M.; Tang, H.; Liu, J.; Yan, F. Rapid and Sensitive Determination of Doxorubicin in Human Whole Blood by Vertically-Ordered Mesoporous Silica Film Modified Electrochemically Pretreated Glassy Carbon Electrodes. *RSC Advances* **2021**, *11* (15), 9021–9028. https://doi.org/10.1039/d0ra10000e.

(17) Keefe, A. D.; Pai, S.; Ellington, A. Aptamers as Therapeutics. *Nature Reviews Drug Discovery* **2010**, *9* (7), 537–550. https://doi.org/10.1038/nrd3141.

(18) Lakowicz, J. R. Quenching of Fluorescence. *Principles of Fluorescence Spectroscopy* **2006**, 277–330. https://doi.org/10.1007/978-0-387-46312-4_8.

(19) Gleichmann, N. *Affinity vs Avidity*. from Technology Networks. https://www.technologynetworks.com/immunology/articles/affinity-vs-avidity-333559.

(20) Schonfeld, S. *Why are some antibodies so expensive?* blog.quartzy.com. https://blog.quartzy.com/why-are-some-antibodies-so-expensive

(21) Kaushal, J.; Singh, G.; Arya, S. K. *Chapter 36 - Emerging trends and future prospective in enzyme technology*. ScienceDirect. https://www.sciencedirect.com/science/article/abs/pii/B9780323899291000366.

(22) Chai, C.; Xie, Z.; Grotewold, E. SELEX (Systematic Evolution of Ligands by EXponential Enrichment), as a Powerful Tool for Deciphering the Protein–DNA Interaction Space. *Methods in Molecular Biology* **2011**, 249–258. https://doi.org/10.1007/978-1-61779-154-3_14.

(23) Wochner, A.; Menger, M.; Orgel, D.; Cech, B.; Rimmele, M.; Erdmann, V. A.; Glökler, J. A DNA Aptamer with High Affinity and Specificity for Therapeutic Anthracyclines. *Analytical Biochemistry* **2008**, *373* (1), 34–42. https://doi.org/10.1016/j.ab.2007.09.007.

(24) Manea, I.; Casian, M.; Oana Hosu-Stancioiu; Noemí de-los-Santos-Álvarez; María Jesús Lobo-Castañón; Cristea, C. A Review on Magnetic Beads-Based SELEX Technologies: Applications from Small to Large Target Molecules. *Analytica Chimica Acta* **2024**, *1297*, 342325–342325. https://doi.org/10.1016/j.aca.2024.342325.

(25) Markham, N. R.; Zuker, M. UNAFold: Software for Nucleic Acid Folding and Hybridization. *Methods in Molecular Biology (Clifton, N.J.)* **2008**, *2* (1), 3–31. https://doi.org/10.1007/978-1-60327-429-6_1.

(26) Jumper, J.; Evans, R.; Pritzel, A.; Green, T.; Figurnov, M.; Ronneberger, O.; Tunyasuvunakool, K.; Bates, R.; Žídek, A.; Potapenko, A.; Bridgland, A.; Meyer, C.; Kohl, S. A. A.; Ballard, A. J.; Cowie, A.; Romera-Paredes, B.; Nikolov, S.; Jain, R.; Adler, J.; Back, T. Highly Accurate Protein Structure Prediction with Alphafold. *Nature* **2021**, *596* (7873), 583–589. https://doi.org/10.1038/s41586-021-03819-2.

(27) Schrödinger, L.; DeLano, W. *The PyMOL Molecular Graphics System, Version~1.8*. PyMol. www.pymol.org/pymol

(28) Rosignoli, S.; Paiardini, A. DockingPie: A Consensus Docking Plugin for PyMOL. *Bioinformatics* **2022**, *38* (17), 4233–4234. https://doi.org/10.1093/bioinformatics/btac452.

(29) Oliveira, R.; Pinho, E.; Barros, M. M.; Azevedo, N. F.; Almeida, C. In Vitro Selection of DNA Aptamers against Staphylococcal Enterotoxin A. *Scientific Reports* **2024**, *14*, 11345. https://doi.org/10.1038/s41598-024-61094-3.

(30) Mayo Clinic. *Hyponatremia - Symptoms and causes*. Mayo Clinic. https://www.mayoclinic.org/diseases-conditions/hyponatremia/symptoms-causes/syc-20373711#:~:text=A%20normal%20blood%20sodium%20level.

(31) Reiff Ellis, R. *What Is a Magnesium Test? Why Do I Need One?* WebMD. https://www.webmd.com/a-to-z-guides/magnesium-test.

(32) Trott, O.; Olson, A. J. AutoDock Vina: Improving the Speed and Accuracy of Docking with a New Scoring Function, Efficient Optimization, and Multithreading. *Journal of Computational Chemistry* **2009**, *31* (2). https://doi.org/10.1002/jcc.21334.

(33) Eberhardt, J.; Santos-Martins, D.; Tillack, A. F.; Forli, S. AutoDock Vina 1.2.0: New Docking Methods, Expanded Force Field, and Python Bindings. *Journal of Chemical Information and Modeling* **2021**, *61* (8). https://doi.org/10.1021/acs.jcim.1c00203.

(34) Leung, K. K.; Gerson, J.; Emmons, N.; Roehrich, B.; Verrinder, E.; Fetter, L. C.; Kippin, T. E.; Plaxco, K. W. A Tight Squeeze: Geometric Effects on the Performance of Three-Electrode Electrochemical-Aptamer Based Sensors in Constrained, in Vivo Placements. *Analyst* **2023**, *148* (7), 1562–1569. https://doi.org/10.1039/D2AN02096C.

(35) National Cancer Institute. *https://www.cancer.gov/publications/dictionaries/cancer-terms/def/peripheral-venous-catheter*. www.cancer.gov. https://www.cancer.gov/publications/dictionaries/cancer-terms/def/peripheral-venous-catheter.

(36) Cowan, D. *Know your oligo mod: Methylene Blue - LGC*. blog.biosearchtech.com. https://blog.biosearchtech.com/know-your-oligo-mod-methylene-blue.

(37) Huang, X.; Duan, C.; Duan, W.; Sun, F.; Cui, H.; Zhang, S.; Chen, X. *Role of electrode materials on performance and microbial characteristics in the constructed wetland coupled microbial fuel cell (CW-MFC): A review Author links open overlay panel*. Science Direct. https://www.sciencedirect.com/science/article/pii/S0959652621011707.

(38) Rowe, A. A.; White, R. J.; Bonham, A. J.; Plaxco, K. W. Fabrication of Electrochemical-DNA Biosensors for the Reagentless Detection of Nucleic Acids, Proteins and Small Molecules. *Journal of Visualized Experiments* **2011**, No. 52. https://doi.org/10.3791/2922.

(39) *Counter Electrode - an overview | ScienceDirect Topics*. www.sciencedirect.com. https://www.sciencedirect.com/topics/chemistry/counter-electrode.

(40) Analytical Sciences Digital Library. *Reference Electrodes*. Chemistry LibreTexts. https://chem.libretexts.org/Bookshelves/Analytical_Chemistry/Supplemental_Modules_(Analytical_Chemistry)/Analytical_Sciences_Digital_Library/Courseware/Analytical_Electrochemistry%3A_Potentiometry/03_Potentiometric_Theory/04_Reference_Electrodes.

(41) Han, K.; Liang, Z.; Zhou, N. Design Strategies for Aptamer-Based Biosensors. *Sensors* **2010**, *10* (5), 4541–4557. https://doi.org/10.3390/s100504541.

(42) Ou, D.; Yan, H.; Chen, Z. An Impedance Labeling Free Electrochemical Aptamer Sensor Based on Tetrahedral DNA Nanostructures for Doxorubicin Determination. *Mikrochimica acta* **2024**, *191* (2). https://doi.org/10.1007/s00604-024-06176-9.

(43) Leung, K. K.; Downs, A. M.; Ortega, G.; Kurnik, M.; Plaxco, K. W. Elucidating the Mechanisms Underlying the Signal Drift of Electrochemical Aptamer-Based Sensors in Whole Blood. *ACS Sensors* **2021**, *6* (9), 3340–3347. https://doi.org/10.1021/acssensors.1c01183.

(44) Ferguson, B. S.; Hoggarth, D. A.; Maliniak, D.; Ploense, K.; White, R. J.; Woodward, N.; Hsieh, K.; Bonham, A. J.; Eisenstein, M.; Kippin, T. E.; Plaxco, K. W.; Soh, H. T. Real-Time, Aptamer-Based Tracking of Circulating Therapeutic Agents in Living Animals. *Science Translational Medicine* **2013**, *5* (213). https://doi.org/10.1126/scitranslmed.3007095.

(45) Downs, A. M.; Gerson, J.; Leung, K. K.; Honeywell, K. M.; Kippin, T.; Plaxco, K. W. Improved Calibration of Electrochemical Aptamer-Based Sensors. *Scientific Reports* **2022**, *12* (1). https://doi.org/10.1038/s41598-022-09070-7.

(46) Zaleskis, G.; Garberytė, S.; Pavliukevičienė, B.; Valinčius, G.; Characiejus, D.; Mauricas, M.; Kraśko, J. A.; Žilionytė, K.; Žvirblė, M.; Pašukonienė, V. Doxorubicin Uptake in Ascitic Lymphoma Model: Resistance or Curability Is Governed by Tumor Cell Density and Prolonged Drug Retention. *Journal of Cancer* **2020**, *11* (22), 6497–6506. https://doi.org/10.7150/jca.46066.

(47) Mage, P. L.; Ferguson, B. S.; Maliniak, D.; Ploense, K. L.; Kippin, T. E.; Soh, H. T. Closed-Loop Control of Circulating Drug Levels in Live Animals. *Nature Biomedical Engineering* **2017**, *1* (5), 1–10. https://doi.org/10.1038/s41551-017-0070.

(48) Watkins, Z.; Karajic, A.; Young, T.; White, R.; Heikenfeld, J. Week-Long Operation of Electrochemical Aptamer Sensors: New Insights into Self-Assembled Monolayer Degradation Mechanisms and Solutions for Stability in Serum at Body Temperature. *ACS sensors* **2023**, *8* (3), 1119–1131. https://doi.org/10.1021/acssensors.2c02403.

(49) Wermuth, C. G. Similarity in Drugs: Reflections on Analogue Design. *Drug Discovery Today* **2006**, *11* (7-8), 348–354. https://doi.org/10.1016/j.drudis.2006.02.006.

(50) Venkatesh, P.; Kasi, A. *Anthracyclines*. PubMed. https://www.ncbi.nlm.nih.gov/books/NBK538187/.

(51) *Doxorubicin*. go.drugbank.com. https://go.drugbank.com/drugs/DB00997.

(52) Bavi, R.; Hang, Z.; Banerjee, P.; Aquib, M.; Jadhao, M.; Rane, N.; Bavi, S.; Bhosale, R.; Kodam, K.; Jeon, B.-H.; Gu, Y. Doxorubicin-Conjugated Innovative 16-Mer DNA Aptamer-Based Annexin A1 Targeted Anti-Cancer Drug Delivery. *Molecular Therapy. Nucleic Acids* **2020**, *21*, 1074–1086. https://doi.org/10.1016/j.omtn.2020.07.038.

(53) ESMO. *Doxorubicin remains the gold standard in the first line chemotherapy for patients with advanced or metastatic soft tissue sarcoma.* www.esmo.org. https://www.esmo.org/meeting-calendar/past-meetings/esmo-congress-2012/News-Press-Releases/Congress-News/doxorubicin-remains-the-gold-standard-in-the-first-line-chemotherapy-for-patients-with-advanced-or-metastatic-soft-tissue-sarcoma#:~:text=No%20difference%20between%20treatment%20arms.